

Supplemental Information

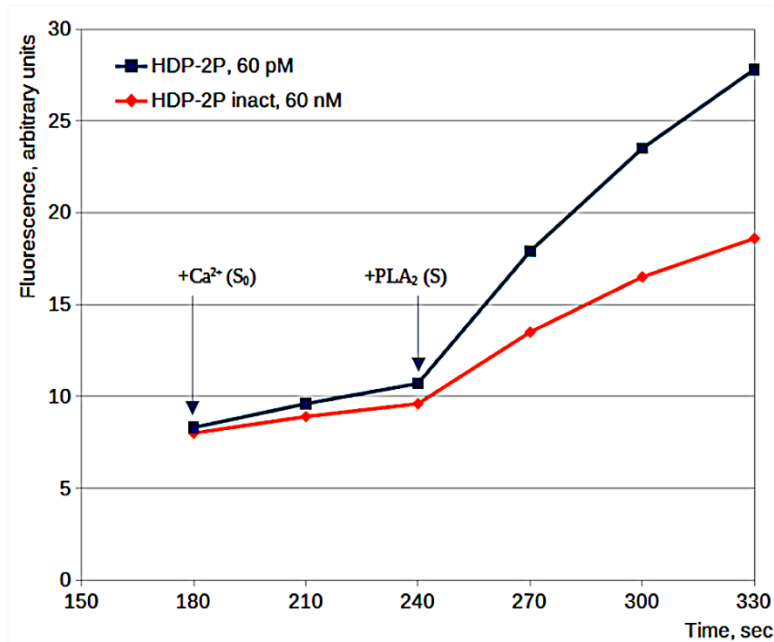


Figure S1. Determination of phospholipolytic activity of HDP-2P (blue line) and HDP-2P inact (red line). This was determined as previously described [Radvanyi et al., 1989]. Fluorescence was recorded every 30 s. The first 180 s was used to establish the level of spontaneous hydrolysis of the fluorescent substrate prior to the addition of calcium chloride. The curves were registered at concentrations of 60 pM and 60 nM for HDP-2P and HDP-2P inact, respectively. Activity (micromoles per minute) was calculated using the formula:

$$A = 2 \times 10^{-4} \times (S - S_0) \times V / F_{\max}$$

where S is the slope of the curve representing the increase of fluorescence versus time (in s); S_0 is the slope observed in the absence of enzyme; V is the volume (in μl) of pyrene phospholipids (0.2 mM) in the reaction medium; and F_{\max} is the maximal fluorescent signal with complete hydrolysis of the substrate. Both V and F_{\max} are equal for HDP-2P and HDP-2P inact. This means that for comparison of activities, we can compare $S - S_0$ values, which are 7.5 and 3.4 for HDP-2P and HDP-2P inact, respectively, i.e. the activity of 60 pM HDP-2P is higher than that of 60 nM HDP-2P inact by 2.2 fold. Considering the three orders of magnitude difference in concentration, we conclude that HDP-2P inact is less active than HDP-2P by 2200 fold.

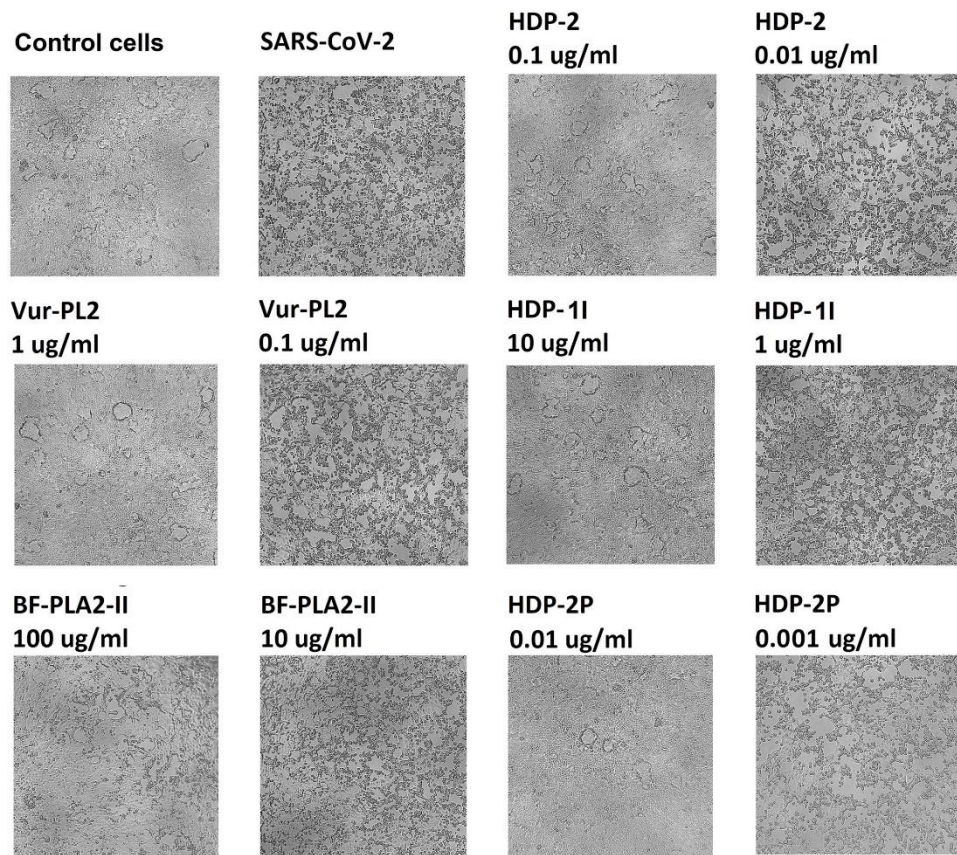


Figure S2. Snake venom PLA₂s prevent the cytopathic effect of SARS-CoV-2 on the Vero E6 cells.

Vero E6 cells were infected with SARS-CoV-2 virus at 100 TCID₅₀ (50% tissue culture infectious dose) in the presence of PLA₂s at the indicated concentrations. The photos were taken 72 h after infection.

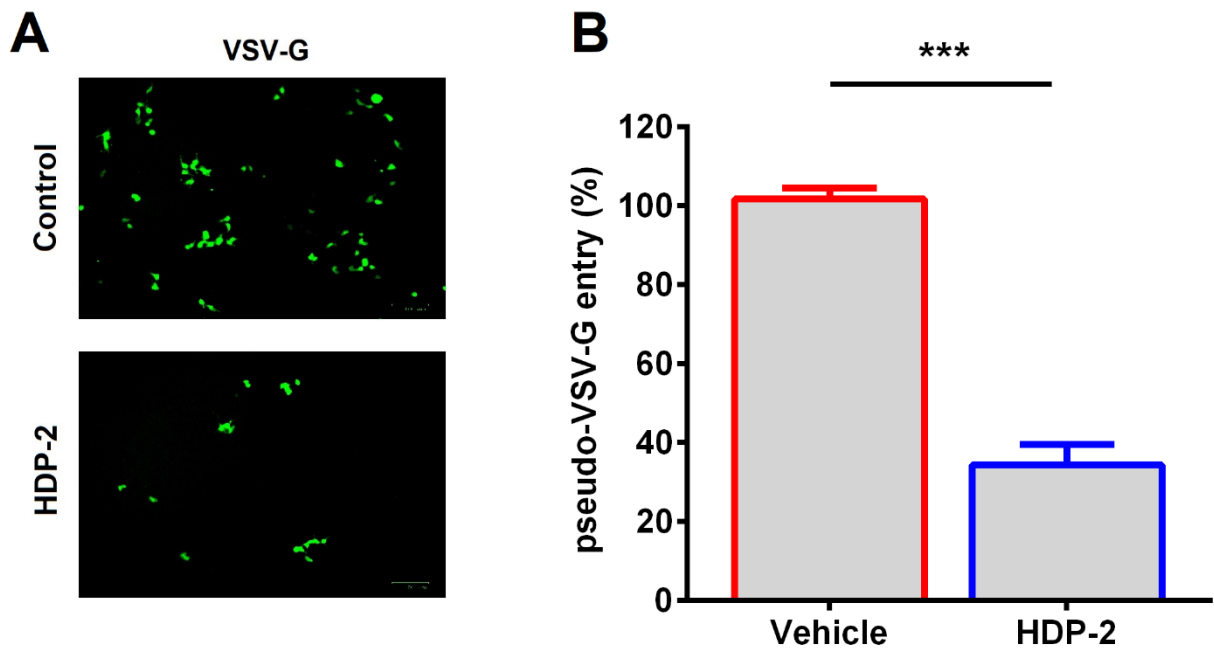


Figure S3. Inhibition of VSV-G pseudovirus entry into cells by HDP-2. 293T/ACE2 were infected with pseudo-VSV-G-GFP either in the presence of vehicle (PBS, Control) or HDP-2 (10 μ g/ml). (A) Representative fluorescent microscopy images of 293T/ACE2 cells infected with the pseudo-VSV-G and treated with HDP-2. Scale bars, 100 μ m. (B) Infectivity of pseudo-VSV-G particles to 293T/ACE2 cells was quantified by measuring the GFP fluorescence. Significant difference was determined using a Student's t-test: *** $p < 0.001$. Results are expressed as means \pm SD. $n = 3$.

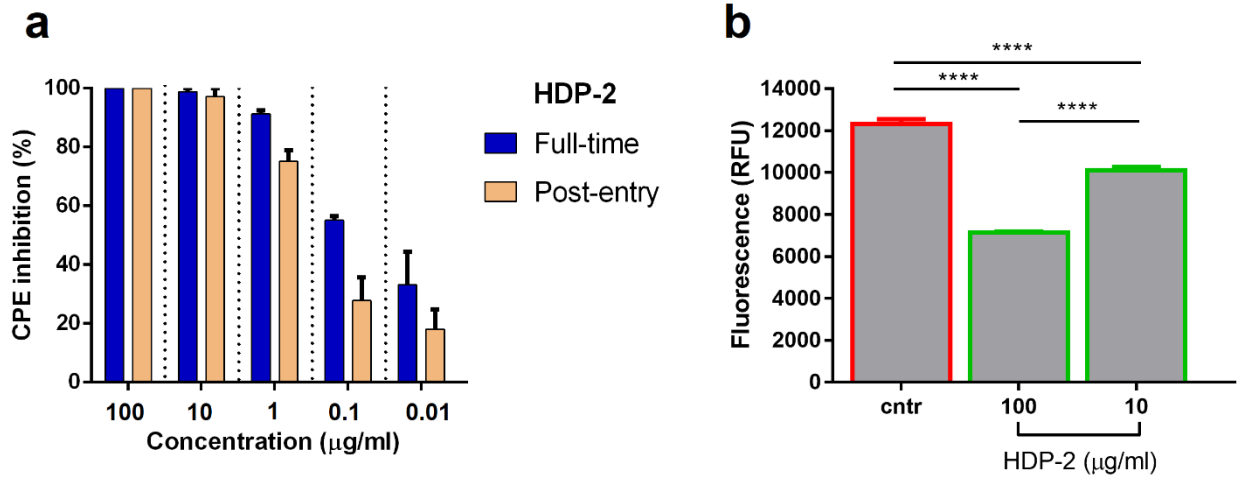


Figure S4. HDP-2 inhibits post-entry stage of live and pseudotyped SARS-CoV-2. (A) Vero E6 cells were infected with SARS-CoV-2 (100 TCID₅₀) for 16 h. Cells were then washed to remove unbound virus, and various concentration of HDP-2 added for 48 h. CPE inhibition was measured by MTT assay. (B) 293T/ACE2 cells were transduced with pseudo-SARS-CoV-2 for 16 h. Cells were then washed and HDP-2 added for 48 h. GFP fluorescence of control and HDP-2 treated 293T/ACE2 cells was measured after 72 h. Data are presented as the mean ± SD. n = 6. One-way ANOVA with Tukey post hoc test was applied to assess statistically significant differences: **** p<0.0001.

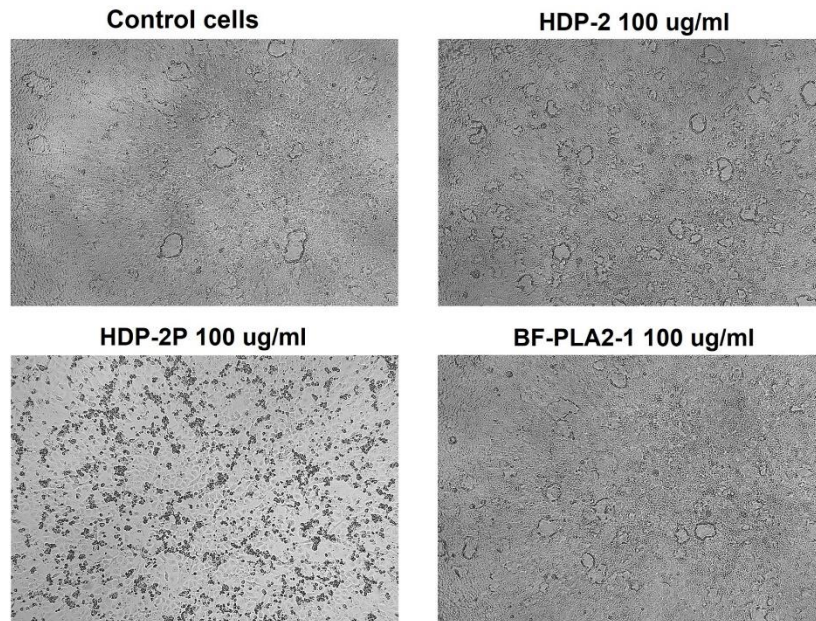


Figure S5. Snake venom PLA₂s effects on Vero E6 cells. The images show the morphology of Vero E6 cells in the presence of various PLA₂s at 100 μ g/ml.

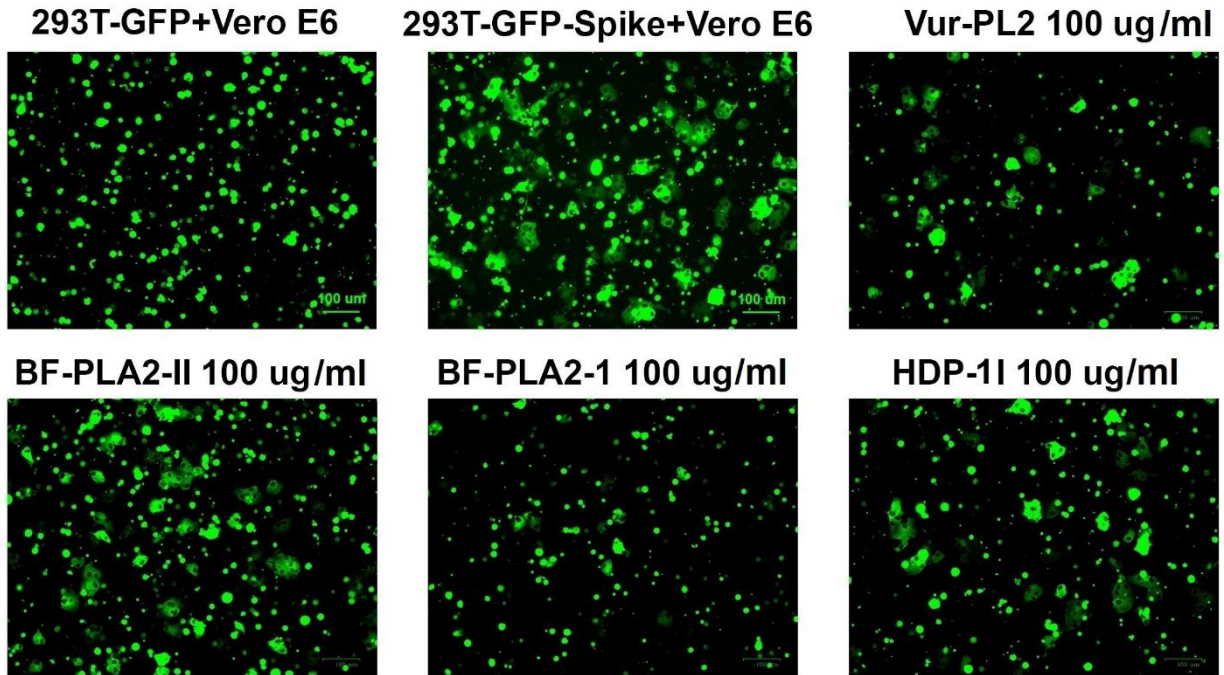


Figure S6. Effects of some PLA₂s on cell-cell fusion mediated by SARS-CoV-2 glycoprotein S. Images of SARS-CoV-2 glycoprotein S mediated cell-cell fusion after a 2 h incubation with different PLA₂s. Scale bar = 100 μm.

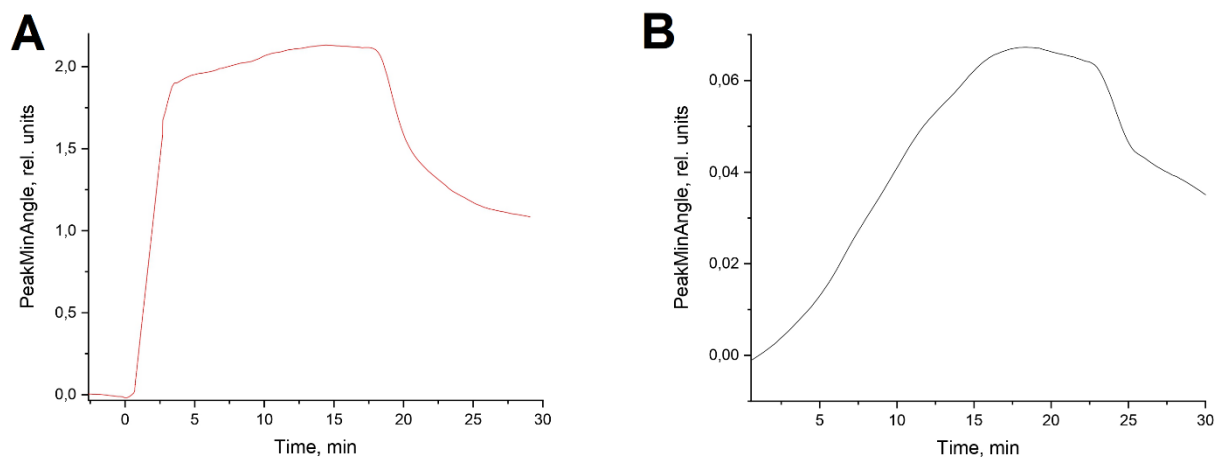


Figure S7. Binding of HDP-2P or RBD SARS-CoV-2 to ACE2. (A) Representative sensorgram for HDP-2P injection into channel with ACE2 (smoothing and curve fitting were applied during processing to eliminate some artifacts caused by the operation of the device). (B) Representative sensorgram for RBD injection into channel with ACE2.